

Dynamics of carriers in resonantly excited quantum-well lasers studied by intersubband absorption

I. Shtrichman,^{a)} U. Mizrahi, D. Gershoni, and E. Ehrenfreund

Physics Department and Solid State Institute, Technion—Israel Institute of Technology, Haifa, Israel

K. D. Maranowski and A. C. Gossard

Materials Department, University of California, Santa Barbara, California 93106

(Received 3 February 2000; accepted for publication 3 April 2000)

Using infrared picosecond pulses to probe the intersubband absorption of GaAs/AlGaAs quantum-well lasers following their optical excitation, we directly measure the dynamics of carriers in these devices. We find no evidence for excitonic gain even at cryogenic temperatures and resonant excitonic excitation. © 2000 American Institute of Physics. [S0003-6951(00)05221-9]

The dynamics of charge carriers and the lasing mechanisms in semiconductor lasers have been very intensively studied for many years.^{1–3} It is commonly accepted that in bulk and heterostructure based semiconductor lasers, stimulated emission and gain is achieved by the creation of electron and hole plasmas for which their individual quasi-Fermi energies separation is larger than the semiconductor fundamental band gap.⁴ However, exciton related mechanisms, such as stimulated emission through annihilation of localized excitons,^{5–7} exciton–exciton interaction or biexciton decay,^{8,9} exciton-optical phonon interaction,¹⁰ and exciton condensation,^{11,12} were also considered.

In this work, we use resonantly tuned visible picosecond (ps) pulse in order to pump the laser sample while the dynamics of the photoexcited electrons is probed by synchronous infrared (IR) pulse which is spectrally tuned into their intersubband transitions. In this photoinduced absorption (PIA) technique, the IR probe pulse induces optical transitions only between photoexcited carrier levels. In marked contrast with the commonly used interband probe pulse,^{1–3} it does not generate electron-hole pairs. Thus, by avoiding the exclusion principle restrictions, it is particularly suitable for testing the lasing mechanism.

The molecular beam epitaxially grown GaAs/Al_{0.33}Ga_{0.67}As semiconductor heterostructure laser devices are schematically described in Fig. 1(b). The active region contains 25 periods of a 6 nm thick layer of GaAs well and a 12 nm thick layer of Al_{0.33}Ga_{0.67}As barrier. Two 1 μm thick layers of Al_{0.5}Ga_{0.5}As surround the active region in order to separately confine the optical mode. In Fig. 1(a) we schematically present the device as prepared for the optical studies. The two edges of the sample were polished at 45° in order to enable intersubband absorption (ISBA) measurements using a *p*-polarized infrared beam.¹³ The substrate was then thinned and 600 μm cavity length laser bars were cleaved perpendicular to the 45° polished surfaces.

The lasers were optically pumped at various excitation densities, I_{ex} , below and above their lasing threshold by an above band gap, spectrally tunable, cavity dumped ps dye laser at a repetition rate of 4 MHz. The induced ISBA was

resonantly probed by a spectrally tuned mid-IR picosecond pulses at a repetition rate of 80 MHz. These frequency difference generated probe pulses are synchronized with the pump pulses. The temporal evolution of the ISBA after the excitation pulse was studied by varying the probe delay time while measuring the transmission through the IR waveguide using 4 MHz lock-in detection.^{13,14} The setup temporal and spectral resolutions are 4 ps and 1 meV (both in the visible and in the IR), respectively.

In Fig. 2 (left scale) we display the emission spectrum along the laser cavity at 20 mW excitation intensity. Dashed (dotted) line shows the spontaneous (stimulated) emission as

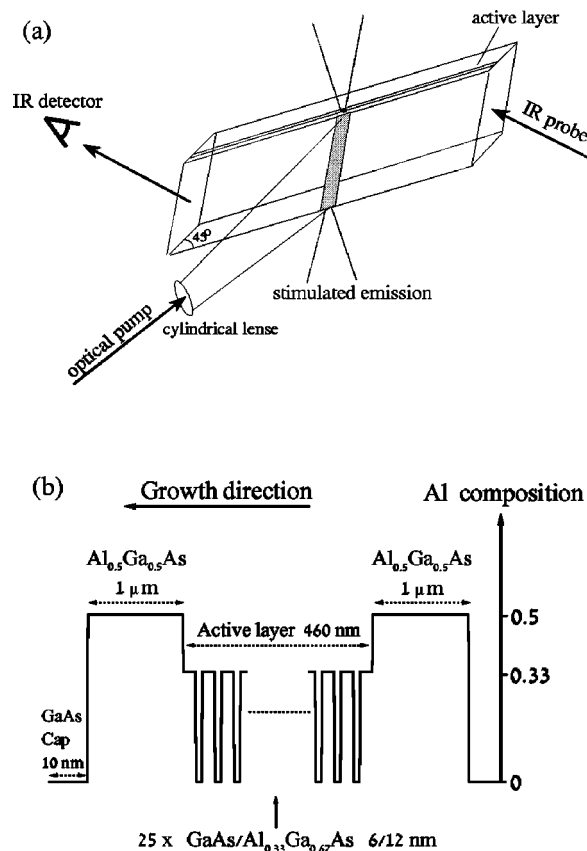


FIG. 1. (a) Schematics of the optical experiment. A visible pump pulse induces lasing along the cavity direction, while the PIA is probed by an IR pulse; (b) the layered structure.

^{a)}Electronic mail: itay@engineering.ucsb.edu

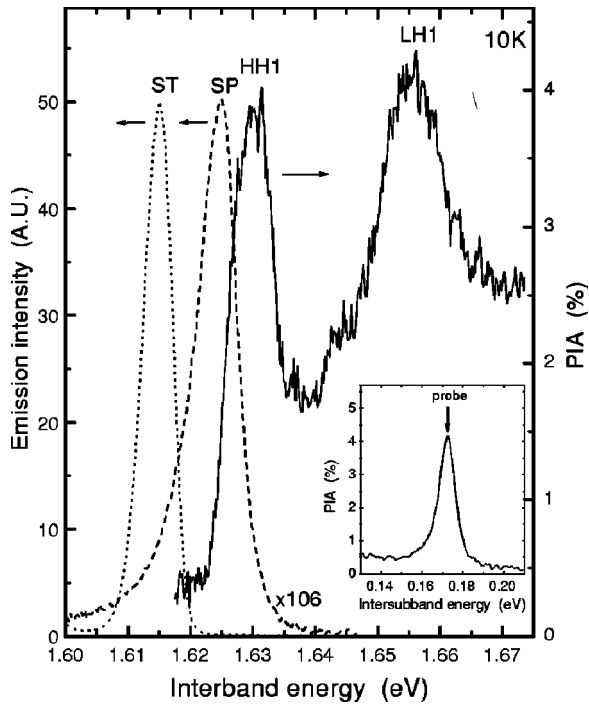


FIG. 2. Above threshold spontaneous (dashed line), and stimulated (dotted line) emission spectra of the laser sample (left scale) together with its PIA excitation (solid line) spectrum (right scale). The inset presents $\int \alpha_{isb} dt$.

measured with the excitation spot elongated parallel (perpendicular) to the laser bar. The temporally integrated photoinduced ISBA, $\int \alpha_{isb} dt$, spectrum of the lasers (inset to Fig. 2) is dominated by the $E1-E2$ electronic transition at 172 meV. The exciting photon energy dependence of the relative intensity of this resonance is presented in Fig. 2 (solid line, right scale). The lowest energy heavy- and light-hole excitonic resonances (HH1 and LH1, respectively) are clearly resolved; we note that the spontaneous (stimulated) emission peaks at 1.625 (1.615) eV, 5 (15) meV below the HH1 resonance. In the following measurements, the laser bars are optically pumped at HH1 and are probed at $E1-E2$. We measure PIA transients at various intersubband spectral positions, and then spectrally integrate them in order to follow the dynamics of the photoexcited electron population.

In the left (center) panel of Fig. 3 we display the spectrally integrated ISBA, $\int \alpha_{isb} dE$, transients for three different I_{ex} under nonlasing (lasing) pump spot orientation. The insets show the temporally and spectrally integrated ISBA, $\int \alpha_{isb} dt dE$, vs I_{ex} . We note that in the nonlasing case, the average electronic population at $E1$, as measured by $\int \alpha_{isb} dt dE$, grows sub-linearly with I_{ex} due to the bleaching of the excitonic resonance at high excitation densities.¹⁵ In this case, $\int \alpha_{isb} dE$ decays exponentially with a single characteristic lifetime of ≈ 300 ps which is almost independent of I_{ex} .

Under lasing conditions (center panel), the three I_{ex} values correspond to threshold (≈ 10 mW, which we estimate to be equivalent to $\approx 4.5 \times 10^{11} \text{ cm}^{-2}$), below threshold (3 mW) and above it (30 mW). We note that below lasing threshold and at long time after the excitation, the ISBA decays with the same characteristic single lifetime, as under the nonlasing conditions. Above threshold, the maximum absorption does not change much with increasing intensity, which is a clear

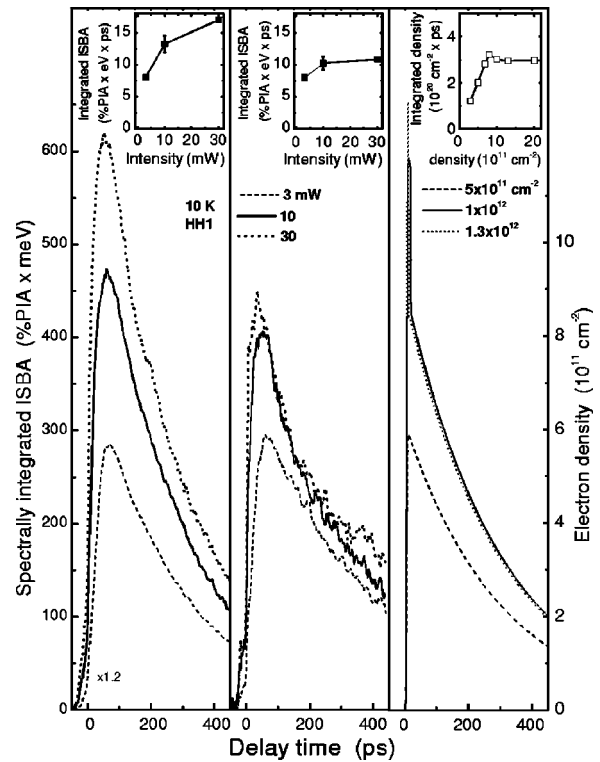


FIG. 3. $\int \alpha_{isb} dE$ vs delay time for three pump intensities. The left (center) panel describes the sample in nonlasing (lasing) pumping configuration, and the right panel describes our model simulations for the lasing configuration. The insets present $\int \alpha_{isb} dt dE$ vs I_{ex} .

indication that the electronic density is clamped to its threshold level. After reaching its maximum, the absorption first rapidly drops, until it reaches a certain level below which it continues to decay characteristically. Similar results were obtained for another sample and also for higher, nonresonant excitation energies.

The dynamic PIA measurements presented in Fig. 3 are a direct measure of the population of $E1$ as the time evolves. As lasing conditions are reached, at or before the end of the pump pulse (≈ 8 ps), $E1$ is forced to depopulate due to the immense number of cavity photons during laser action. Therefore, the maximum of the ISBA is almost unchanged above threshold. After the electron density drops below threshold (at ≈ 50 ps), the depopulation of $E1$ is still rapid due to yet quite strong stimulated emission. When the electron density drops further (at ≈ 150 ps), the population inversion as well as the photon density decrease, leading to spontaneous emission only during the last temporal decay stage. We have quantitatively simulated the transient behavior of the short optical pulse pumped quantum well laser using a simple two coupled rate equations model. We have assumed electron and hole plasmas with a single lasing mode and spatially independent densities:¹⁶

$$dN/dt = R - N/\tau - v_g g n_{ph}, \quad (1)$$

$$dn_{ph}/dt = -n_{ph}/\tau_c + \Gamma v_g g n_{ph}, \quad (2)$$

where $N(t)$ [$n_{ph}(t)$] is the $E1$ electron (cavity photon) density, and $R(t)$ represents a Gaussian shaped pump pulse centered at zero time with FWHM=4 ps. The confinement factor, dictated by the well to barrier thickness ratio is $\Gamma = 0.33$, and the group velocity of light in the active layer is

$v_g = 0.66 \times 10^{10}$ cm/s.¹⁶ The gain, $g(N)$, as a function of the carrier density at 10 K is calculated using an eight band $\mathbf{k} \cdot \mathbf{p}$ model.¹⁷ The $E1$ electron population spontaneous lifetime is $\tau = 300$ ps, as directly deduced from our measurements (Fig. 3). τ_c is the photon lifetime in the cavity. It depends on the photon round-trip time, $T = 2nL/c$, and on the mirror reflections (R_1, R_2) and cavity loss (α_0): $\tau_c = T/[2\alpha_0L - \ln(R_1R_2)] = 6$ ps.

The calculated electron density as a function of time for the estimated experimental I_{ex} is presented in Fig. 3 (right panel). In general, our simple model calculations quantitatively describe the experimental measurements. In particular the ‘‘clamping’’ of the carrier density to its threshold density by the stimulated emission¹⁸ is quantitatively reproduced (see inset). In one detail, however, there is a significant deviation between the experiment and model. The calculations give a temporally short (≈ 1 ps) significant increase in the carrier density when it reaches threshold, and before the increasing photon density force it back to its threshold value. This behavior was not observed experimentally, probably due to lack of temporal resolution.

In summary, using a unique time-resolved optical technique, we are able to directly measure the dynamics of carriers in resonantly optically pumped GaAs/AlGaAs quantum well lasers. We find that lasing starts at the end of the resonant excitation pulse and that it lasts for about 40 ps. During lasing the carrier density is almost clamped to its threshold value. Our theoretical analysis yields that even at the favorable conditions of cryogenic temperature and resonant excitonic excitation, there is no indication for excitonic gain in these devices.

The work was supported by the Israel Science Foundation founded by the Israel Academy of Sciences and Humanities.

- ¹T. Takahashi, M. Nishioka, and Y. Arakawa, Appl. Phys. Lett. **58**, 4 (1991).
- ²P. Michler, A. Lohner, W. W. Ruhle, and G. Reiner, Appl. Phys. Lett. **66**, 1599 (1995).
- ³F. Sogawa, A. Hangleiter, H. Watabe, Y. Nagamune, M. Nishioka, and Y. Arakawa, Appl. Phys. Lett. **69**, 3137 (1996).
- ⁴A. Yariv, *Quantum Electronics*, 3rd ed. (Wiley, New York, 1989).
- ⁵J. Ding, H. Jeon, T. Ishihara, M. Hagerott, A. V. Nurmikko, H. Luo, N. Samarth, and J. Furdyna, Phys. Rev. Lett. **69**, 1707 (1992).
- ⁶K. B. Ozanyan, J. E. Nicholls, M. O'Neill, L. May, J. H. C. Hogg, W. E. Hagston, B. Lunn, and D. E. Ashenford, Appl. Phys. Lett. **69**, 4230 (1996).
- ⁷X. Fan, H. Wang, H. Q. Hou, and B. E. Hammons, Phys. Rev. B **56**, 15256 (1997).
- ⁸F. Kreller, M. Lowisch, J. Puls, and F. Henneberger, Phys. Rev. Lett. **75**, 2420 (1995).
- ⁹V. Kozlov, P. Kelkar, A. Vertikov, A. V. Nurmikko, C.-C. Chu, J. Han, C. G. Hua, and R. L. Gunshor, Phys. Rev. B **54**, 13932 (1996).
- ¹⁰I. Galbraith and S. W. Koch, J. Cryst. Growth **159**, 667 (1996).
- ¹¹P. B. Littlewood and X. Zhu, Phys. Scr. T **68**, 56 (1996).
- ¹²H. Chu and Y. C. Chang, Phys. Rev. B **54**, 5020 (1996).
- ¹³R. Duer, I. Shtrichman, D. Gershoni, and E. Ehrenfreund, Phys. Rev. Lett. **78**, 3919 (1997).
- ¹⁴R. Duer, D. Gershoni, and E. Ehrenfreund, Superlattices Microstruct. **17**, 5 (1995).
- ¹⁵S. Schmitt-Rink, D. S. Chemla, and D. A. B. Miller, Adv. Phys. **38**, 89 (1989).
- ¹⁶L. A. Coldren and S. W. Corzine, *Diode Lasers and Photonic Circuits* (Wiley, New York, 1995).
- ¹⁷D. Gershoni, C. H. Henry, and G. A. Baraff, IEEE J. Quantum Electron. **29**, 2433 (1993).
- ¹⁸T. Paoli, IEEE J. Quantum Electron. **9**, 267 (1973).